Proceedings of the XXVI Iberian Latin-American Congress on Computational Methods in Engineering CILAMCE 2005
Brazilian Assoc. for Comp. Mechanics & Latin American Assoc. of Comp. Methods in Engineering
Guarapari, Espírito Santo, Brazil, 19^{th}–21^{st} October 2005

Paper CIL14-813

Numerical Meshes from Seismic Images

Karl Apaza Agüero, Paulo Roma Cavalcanti, Antonio Oliveira, Claudio Esperança
{*karl,roma,oliveira,esperanc*}*@lcg.ufrj.br*
LCG-Computer Graphics Laboratory, UFRJ-COPPE
Cidade Universitária-Ilha do Fundão, Rio de Janeiro - RJ - Brazil

Abstract. *This work implements a methodology for the creation of numerical meshes from seismic images, which does not require, in theory, human intervention. The main goal is to adapt the mesh generation techniques in order to directly process digital images obtained by seismic survey. Traditionally, such images must first be examined by geologists and geophysicists who, in turn, model the fundamental geometric shapes, i.e., horizons and faults. The proposed technique generates meshes directly from the seismic images, by combining image processing and physical modeling. Horizons and faults are therefore extracted directly from the mesh, instead of being obtained from an intermediate geometrical model.*

Keywords: *Horizons and faults, Enhancement of features, Physical models*

1. INTRODUCTION

The simulation of complex geological processes such as the evolution of sedimentary basins and multiphase fluid flow within sediments is important for decision-making processes in the oil industry. In oil exploration and production, critical decisions are made based on the results of reservoir-scale or basin-wide simulations. The quality of these simulations is directly dependent on the accuracy of subsurface earth models.

The drilling of a wildcat well can cost between $ 5 to 50 million USD. The worldwide success rate of these wells is on average less than 10%. In known petroleum reservoirs, an average of 40% is recovered or produced, whereas about 35% of the oil is usually left in place due to rock-fluid interaction forces. The remaining 25% can be potentially recovered and may represent a sizable increase of assets for oil companies if new technologies, to identify and produce these resources, are made available.

One of the major causes of the relatively poor performance in exploration and production is the limited knowledge of the physical and geometrical characteristics of earth models. The construction of earth models is a phenomenal problem not only due to the scarcity of data but because of the geometrical complexity of geological structures. The major sources of subsurface data comes from wells and from interpretation of the acoustic response to seismic waves. This data is very patchy in nature and provides a limited amount of information for building the earth model ”puzzle”.

Traditionally, the geological interpretation of seismic images results in a set of curves and surfaces, which are used to construct a consistent earth model. This model can then be used to generate discrete meshes for several kinds of numerical simulations, such as a reservoir simulation, the propagation of acoustic waves, or large-scale fluid and heat flow within saturated porous sediments.

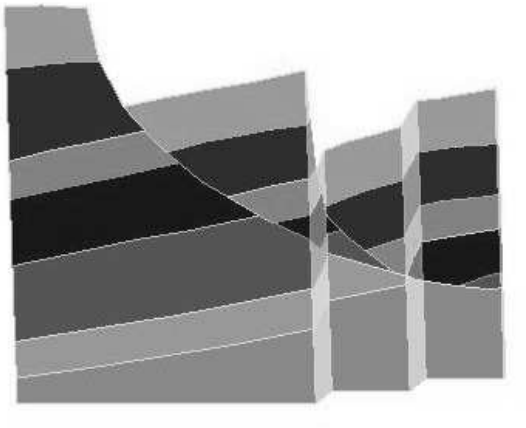

Figure 1: Horizons and geological faults.

The geological model must contain all of the important features, such as horizons (separating surfaces between geological layers) and faults (discontinuities caused by the sliding of layers), as can be seen in Figure 1. Horizons and faults compart the geological model in a set of regions of the space, the union which generates the layers. The geological model is used to create a numerical mesh, which contains the boundary of the model. Horizons and faults are represented as faces of tetrahedra in 3D, or edges of triangles in 2D.

A different approach, created by Hale (Hale, 2001, 2002), adapts Image Processing techniques and physical modeling, in order to create meshes (containing horizons and faults) directly from seismic images, without creating an intermediate geometric model, as can be seen in Figure 2(a). Therefore, horizons and faults are extracted directly from the mesh producing a fully automated processing sequence.

In this work we describe an approach related to Hale's, but we created a pre-processing scheme that produces more adequate input images from a given seismic. The process begins by enhancing horizons and faults in the seismic image, and generating an initial lattice of points (atoms) over the domain of the model. Then, it associates a potential energy to the image pixels and to the atoms of the lattice. Using the lattice, the atoms are moved to a configuration of minimum potential energy, and a mesh is generated by means of a Delaunay triangulation. The horizons and faults from the seismic are present in the mesh as edges (in 2D) or faces (in 3D), as can be seen in Figure 2(b).

2. PHYSICAL CONCEPTS

A seismic image usually depicts a set of curves and surfaces, which act as layer boundaries. Several physical models have been proposed recently, which aim at computing optimal positions for points on those boundaries, producing good results (Jalba et al., 2004; Costa, 1999; Shimada, 1993; M. H. Garcia and Aziz, 1992).

Active contours (Kass et al., 1988; McInerney and Terzopoulos, 1995), for instance, are a class of algorithms known to properly segment images in many applications where the boundaries are not well established. However, they are not applicable in our case due to the large number of thin and disconnected features, presented in a typical seismic

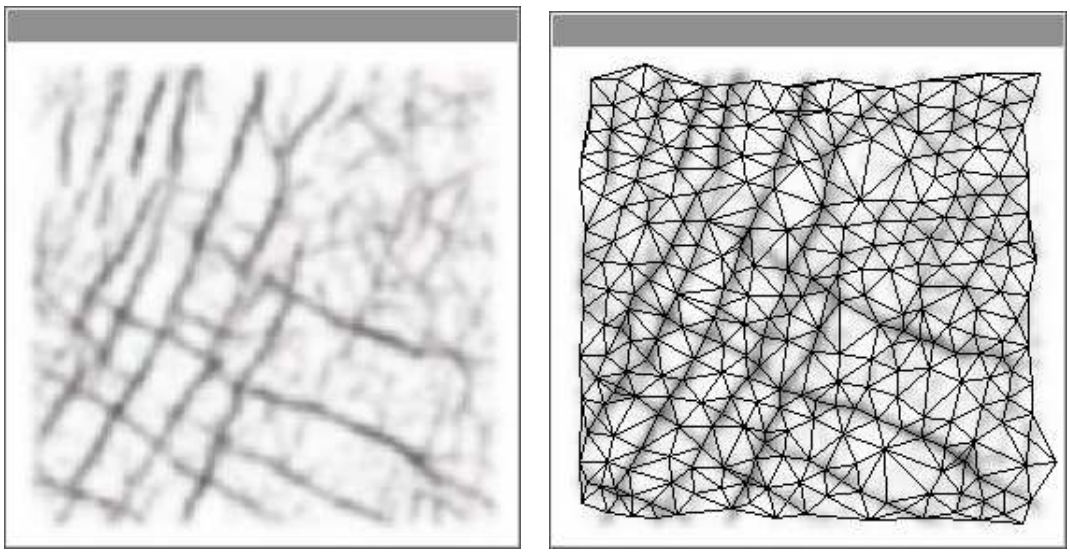

(a) (b)

Figure 2: (a) Seismic image. (b) Final mesh.

image. A different snake should be initialized for each region delimited by a set of linear features. As some of the regions have complex shapes, including narrow bottlenecks, it is not possible to guarantee that long extensions of the feature borders are not lost at the end of the process. Moreover, even if topologically adaptive snakes (implicit or not) are used, it is likely that different features are aggregated in a same contour. A post-processing is then required to separate them, in this case. The snake displacement in a given step must also be small enough so that it does not not jump over a whole feature, which slows down the process.

Some applications using physical models have been implemented (Hale, 2001, 2002), and the trick is how to pre-process the seismic so the resulting image can be used as input for a point optimizer.

2.1 Atom

An atom is a point in the image subjected to forces exerted by its neighbors closer than a limit distance, D, as can be seen in Figure 3. An inter-atomic force must satisfy the following conditions:

a) Be null beyond a predefined distance, to limit the zone of influence of an atom.

b) Be a continuous function of the inter-atomic distance.

c) Be repulsive (positive) to avoid atoms very close to each other. In the same way, to avoid large empty spaces, the force among two atoms must be attractive (negative) whenever the atoms are far away from each other.

From the last condition, we call nominal distance, d, the minimum distance at which the repulsive and the attractive forces are equal.

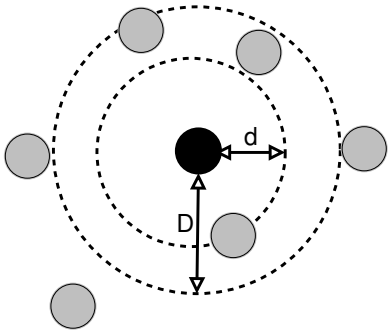

Figure 3: Interaction between atoms.

2.2 Force function between pairs of atoms

We model the interaction force between atoms as a piecewise polynomial function (Shimada, 1993), Eq. (1):

$$f(u) = \left\{ \begin{array}{ll} \frac{9}{8} - \frac{19}{8}u^2 + \frac{5}{4}u^3, & 0 \leq u < \frac{3}{2} \\ 0, & \frac{3}{2} \leq u \end{array} \right\}, \tag{1}$$

where d is the nominal distance of an atom, and u the normalized distance defined by Eq. (2):

$$u = \frac{|x_i - x_j|}{d}. \tag{2}$$

Note that the force is positive in the range [0.0,1.0), negative in the range [1.0,1.5), and zero elsewhere. The total force exerted onto an atom by its neighbors is the sum of all forces exerted by each one of them.

Generally, the force onto an atom is a vector. The direction of this vector is given by the sign of $f(u)$, and by the positions x_i and x_j of two atoms. Nonetheless, it is also possible to define the force as the negative of the gradient of an scalar potential, Eq. (3), which permits the problem to be solved by means of minimization techniques.

$$\phi(u) = \left\{ \begin{array}{ll} \frac{153}{256} - \frac{9}{8}u + \frac{19}{24}u^3 - \frac{5}{16}u^4, & 0 \leq u < \frac{3}{2} \\ 0, & \frac{3}{2} \leq u \end{array} \right\}. \tag{3}$$

2.3 Fields and Potential Energy

We define the atomic potential energy, A, as the sum of the potential field of each atom in the system, and the potential field of an atom is the sum of the forces exerted onto it by its neighbors, Eq. (4):

$$A = A(x_1, x_2, ..., x_n) = \frac{1}{2}\sum_{i=1}^{n}\sum_{j=1, j\neq i}^{n} \phi[\frac{|x_i - x_j|}{d(x_j)}], \tag{4}$$

where $x_1, x_2, ..., x_n$ are the coordinates of n atoms, and $d(x_j)$ the nominal inter-atomic distance function of an atom j.

The image potential energy, B, is defined as the sum of the atomic potential fields associated to image points. The potential field of a point, $b(x_i)$, is just the pixel value (grey scale level) associated to the image, Eq. (5).

$$B = B(x_1, x_2, ..., x_n) = \sum_{i=1}^{n} b(x_i). \tag{5}$$

The total potential energy, P, is the weighted sum of the atomic potential energy, and the image potential energy, Eq. (6):

$$P = P(x_1, x_2, ..., x_n) = (1 - \beta)A + \beta B, \tag{6}$$

where the scale factor β determines the contribution of A and B to the total of potential energy, P. When $\beta = 0$, the atoms create a regular lattice, not necessarily aligned to the important features of the image. When $\beta = 1$, the atoms are sensitive only to the features of the image, producing an irregular lattice.

3. METHODOLOGY

Based on physical models and the work of Hale (Hale, 2002, 2001), we propose an algorithm to create meshes satisfying the important features of an image. The algorithm can be summarized by the steps below:

a) Enhancement of the important features.

b) Generation of an initial lattice of atoms based on the important features.

c) Minimization of the total potential energy function.

d) Generation of a Delaunay triangulation using the lattice of atoms.

4. ENHANCEMENT OF THE IMPORTANT FEATURES

The pre-processing of the input image is necessary because the alignment of the mesh depends on the detection of the important features in the image.

Geological applications created to perform boundary detection employ numerous filters to detect seismic faults (T. Randen and Sonneland, 2001; D. Gibson and Turner, 2003). However, these filters do not always produce the adequate enhancement of the important features to allow the automation of the whole process for images in general (including the mesh generation from the seismic).

Therefore, to allow the automation of this process are used two known image processing techniques:

1) Sobel operators for boundary detection.

2) Morphological operators for enhancement and suppression of irrelevant features from the image.

4.1 Boundary detection

A boundary detector is used to identify image features in the image. The main goal is to differentiate and smooth the original image.

A very common boundary detector is based on the gradient. The gradient vector points in the direction of the steepest variation of the image at a point. In boundary detection, the magnitude of the gradient vector is approximated by absolute values (Gonzales and Woods, 1992), as in Eq. (7):

$$|\nabla f| = |G_x| + |G_y| \,, \tag{7}$$

where ∇f is the gradient of the image at position (x, y).

The gradient of an image is based on the partial derivatives at position (x, y), and can be obtained by the Sobel operators. These operators offer the advantage of providing the desired effects of differentiation and smoothing. Since derivation increases the noise, smoothing is a particularly attractive facet of the Sobel operators.

From equation (7), the derivatives, based on the Sobel operator mask, Eq. (8), are:

$$\begin{aligned} G_x &= (z_7 + 2z_8 + z_9) - (z_1 + 2z_2 + z_3) \\ G_y &= (z_3 + 2z_6 + z_9) - (z_1 + 2z_4 + z_7), \end{aligned} \tag{8}$$

where z are the levels of grey of the pixels covered by the mask (9) at any position of the image:

$$\begin{matrix} z_1 & z_2 & z_3 \\ z_4 & z_5 & z_6 \\ z_7 & z_8 & z_9 \end{matrix} \tag{9}$$

4.2 Boundary enhancement

Another desirable effect in the image pre-processing is the suppression of irrelevant data from the image, while preserving its essential features. Dilation and erosion of features of the image are important to our algorithm.

The implemented morphological operators of dilation and erosion can grow or reduce shapes, respectively. The process is based on the features of the image, and can be changed accordingly to the purposes of each application.

The dilation is the morphological transformation that combines two matrices trough vector addition of its elements. Formally, the dilation of X by Y, denoted by $X \oplus Y$, is defined by Eq. (10):

$$X \oplus Y = \{z \in E^N | z = x + y,\ x \in X,\ y \in Y\}, \tag{10}$$

where X is the matrix of the image being morphologically processed, and Y is the structuring element. Every point of the form $E^N (N = 2)$, corresponding to the translation of points of an object X by elements of Y, belong to the dilated image. There is, X is scanned by Y. Every time the origin Y is superimposed onto a point of X, it is executed an OR of the set Y translated with the final image.

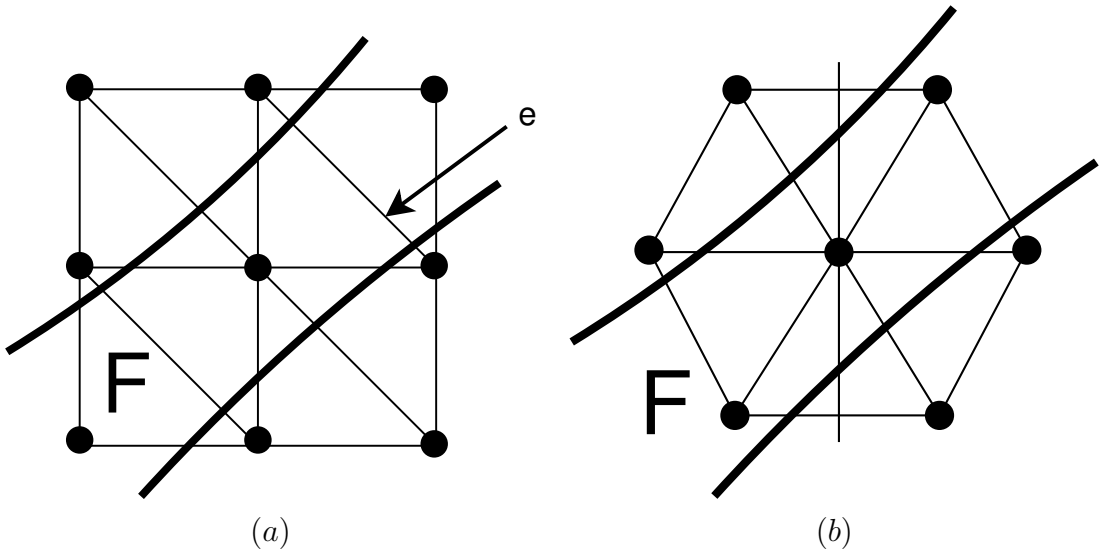

Figure 4: (a) Rectangular lattice. (b) Hexagonal lattice.

Erosion is the morphological dual of dilatation, which is the morphological transformation that combines two matrices by the relation "is contained". Formally, the erosion of X by Y, denoted by $X \ominus Y$, is defined by Eq. (11):

$$X \ominus Y = \{z \in E^N | z + y \in X, \forall y \in Y\}. \tag{11}$$

Figure 7(a) depicts the result of the application of erosion in the seismic image.

5. GENERATION OF AN INITIAL LATTICE OF ATOMS

After the pre-processing of the image, when the features have been already detected and enhanced, it is possible to start the generation of an initial lattice of atoms.

Since the total potential energy, P, is a function of the atom coordinates, it may possess many local minima, because it is a non-quadratic function. The optimization of the potential energy, P, means to find some local minima from the initial lattice, which must have the following characteristics:

a) minimize the atomic potential energy,

b) be regular and

c) be consistent with the nominal distance function.

A constant nominal distance function allows a simple generation of an initial regular lattice of points, holding the previous properties. A rectangular lattice, where the edge length is the nominal distance, is the simplest choice. An hexagonal lattice (Ville et al., 2004) is a better solution, though, for an initial lattice of points, mainly when the image presents important features very thin. In Figure 4(a), there is a rectangular lattice with an

edge length equal to the nominal distance, and an image with a feature, F, whose width is in the range $[d, d\sqrt{2}]$. If the image is approximated by linearly interpolating its node values, no transition will occur along edge e. However, if an hexagonal lattice (Figure 4(b)) is used, every edge crossed by F connects an interior to an exterior point of F. Therefore, transitions will occur in this case. Furthermore, in many cases, the hexagonal lattice is the best solution to automated processes in the generation of seismic meshes.

A variable distance function poses some difficulties, as pointed out by Hale(Hale, 2001). Nonetheless, he suggests an algorithm,(Figure 5), to create a pseudo-regular lattice of atoms, which is adequate to images possessing thick features.

```
Make an array of boolean flags, w(x) = false
Create an empty list of atoms
Create an empty queue of atom positions
Add to the queue the position of the image centre
While the queue is not empty {
   Get, and remove from the queue, the first position x_i
   If x_i is onto the image limits {
      Make an sphere with centre x_i and diametre αd(x_i)
      If the sphere contain positions with w(x) = false {
         Do for all positions inside the sphere
            w(x) = true;
         add to the list
          an atom with coordinates x_i;
         add at the end of the queue
          ideal positions for neighbors;
      }
   }
}
```

Figure 5: Pseudo-code for the pseudo-regular lattice.

The factor α is the proportionality constant that allows some atoms of the initial lattice to get closer than their respective nominal distances. The positions of the neighbors of the atom, removed from the queue, should be, ideally, a function of the width of the image features. The hexagonal lattice generated on the seismic image can be seen in Figure 7(b).

6. TOTAL POTENCIAL ENERGY FUNCTION MINIMIZATION

After the generation of the initial lattice, the atoms must be moved to a configuration that minimizes the total potential energy, P. The descendent gradient is used to minimize the potential energy function, which possesses many local minima. Therefore, the search must be repeated until the most adequate minimum is found. The algorithm (Figure 6), is used to optimize the lattice of atoms (Hale, 2001).

Get the initial lattice with coordinates $x_1, x_2, ..., x_n$
Compute the total potential energy, P, of the initial lattice
Do {
    $P_0 = P$
    Disturb randomly $x_1, x_2, ..., x_n$
    Do {
        $P_i = P$
        Minimize, P, adjusting $x_1, x_2, ..., x_n$
    } While $P_i - P > \epsilon |P_i|$
} While $P_0 - P > \epsilon |P_0|$

Figure 6: Pseudo-code for the optimized lattice.

The threshold ϵ controls the iterations, until the decreasing in P is insignificant. Figure 7(c), depicts the final optimized lattice.

7. GENERATION OF A DELAUNAY TRIANGULATION

The optimized lattice of atoms is structured using a Delaunay triangulation. After the lattice optimization, the density of atoms is greater along the features of the image. The Delaunay triangulation has been, therefore, chosen because it always connects closest points (atoms). The Delaunay triangulation creates edges (in 2D) and faces (in 3D) aligned to the features of the image, as shown in Figure 7(d).

An extension of our methodology can be obtained by means of a post-processing of the mesh to segment it. Cuadros proposes an algorithm (Cuadros and Nonato, 2004) that groups adjacent triangles based on their color pattern. In (Hale and Emanuel, 2004) there is a seismic survey using a global image segmentation, by means of a stochastic algorithm (Y. Gdalyahu and Werman, 2001).

8. RESULTS AND CONCLUSIONS

Figure 8(a) presents a continental seismic from America, Europe and Asia. Two morphological transformations of erosion, and one of dilation, have been applied during the image pre-processing. The resulting image was used to create an initial hexagonal lattice with a nominal distance of 10 pixels. The lattice has been optimized using a nominal distance of 10 and 20 pixels. The aligned and segmented meshes can be seen in Figures 8(b) and 8(c), respectively.

Figure 9 shows the use of the methodology in a 3D seismic image. The 3D block is part of the seismic data of the Stratton field, in the south of Texas (A. Raymond and Pendleton, 1994). In the 3D image pre-processing, there have been applied morphological transformations of dilation and erosion. This image has been used to create an initial hexagonal lattice with a nominal distance of 10 pixels (due to the thin features of the image). The minimization of the lattice potential energy used a nominal distance of 9 to 27 pixels. To show the alignment of the mesh with horizons and faults, there have been

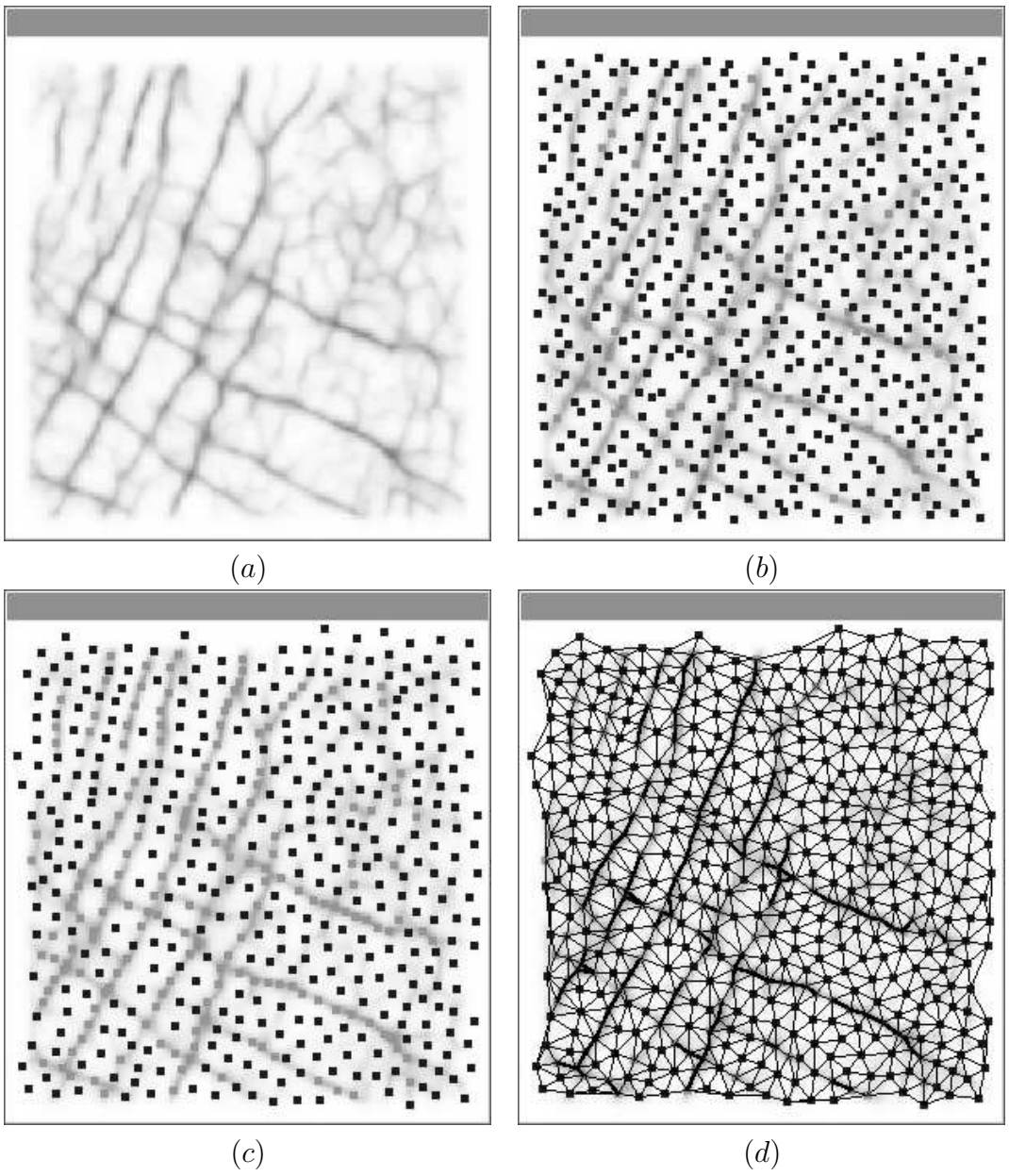

Figure 7: (a) Seismic image with 255 levels of grey. We used erosion operator to supress the noise. (b) Initial hexagonal lattice generated on the image by means of a nominal distance of 6 and 12 pixels, and a scale factor β of 0.5. (c) Optimized lattice with a nominal distance of 6 pixels for atoms onto faults (black), and a nominal distance of 12 pixels for the other atoms (white). It was also used a random disturbance of 20% of the nominal distance value, and a threshold ϵ of 0.001. (d) Delaunay triangulation created by CGAL (Geometry Factory, 2004), with edges aligned to faults.

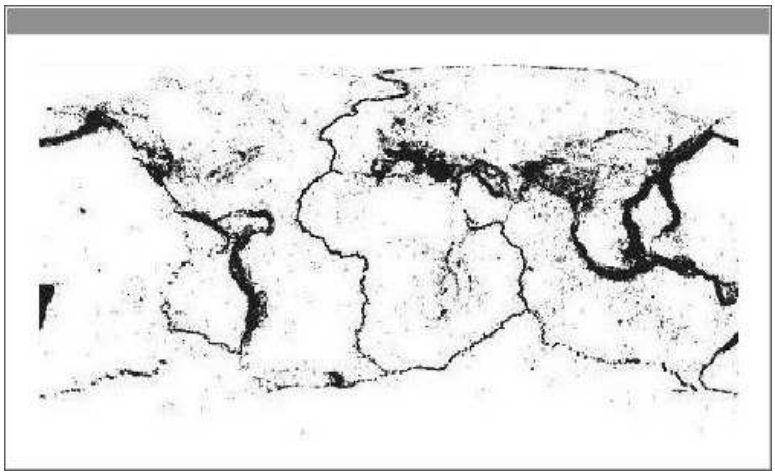

(a)

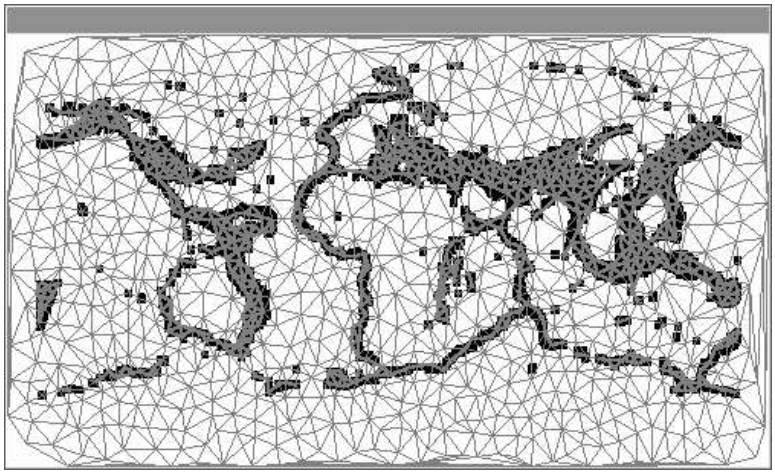

(b)

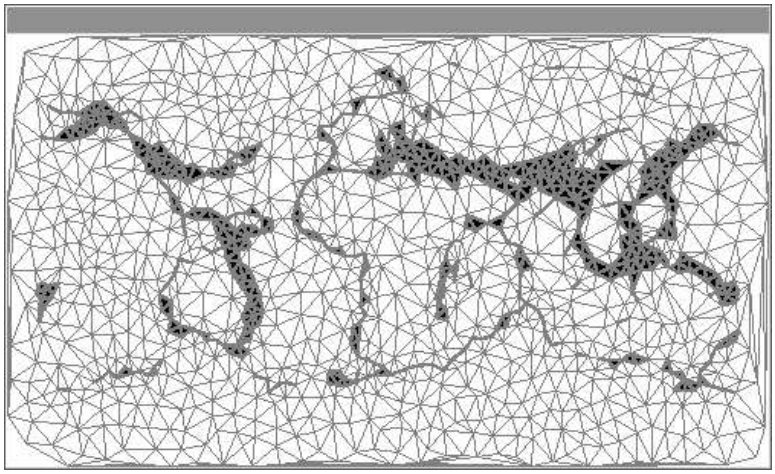

(c)

Figure 8: (a) Continental seismic. (b) Mesh aligned to the continental image. (c) Segmented mesh.

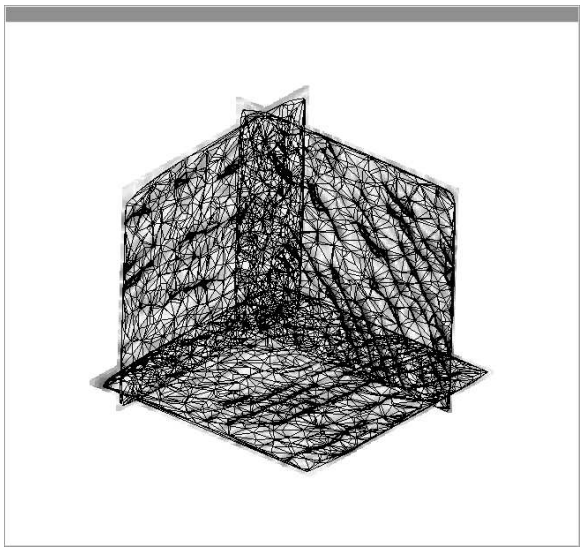

Figure 9: Mesh aligned to the 3D seismic image.

made three orthogonal cuts. Each cut shows the intersection of tetrahedra with a cutting plane.

Alternatively, atoms can be structured, using Voronoi Diagram, by simply changing the sign of the image, $b(x_i)$. Figure 10 presents a Voronoi polygonal mesh using the same parameters of Delaunay triangulation created from figure 2(a). Here Voronoi polygons are generated with edges aligned to horizons and faults on the seismic image.

Enhancement of important features is fundamental in the presented methodology, so any point optimizer tends to produce reliable results. In practice, a seismic should be filtered many times prior to the analysis carried out by a geologist or geophysicist. The automation of the process also depends on a filtered image, and the result strongly depends on the set of filters applied. It is expected that the set of faults and horizons compart the image into a set of regions, which are going to compose the geological layers. However, if the input image does not permit the obtaining of closed regions, maybe because it has not been filtered appropriately, the methodology will not be able to close "the holes". Nevertheless, the methodology can be used, in many other applications, to segment images in general.

REFERENCES

A. Raymond, B. Hardage, R. E. & Pendleton, V., 1994. 3-d seismic and well log data set. fluvial reservoir systems, stratton field, south texas. *Bureau of Economic Geology*.

Costa, L., 1999. Particle systems analysis by using skeletonization and exact dilations. *Particle and Particle System Characterization*, vol. 16, n. 6, pp. 273–277.

Cuadros, A. & Nonato, L., 2004. Geração de malhas Delaunay bidimensionais a partir de imagens. In *XXV CILAMCE Iberian Latin American Congress on Computational Methods*.

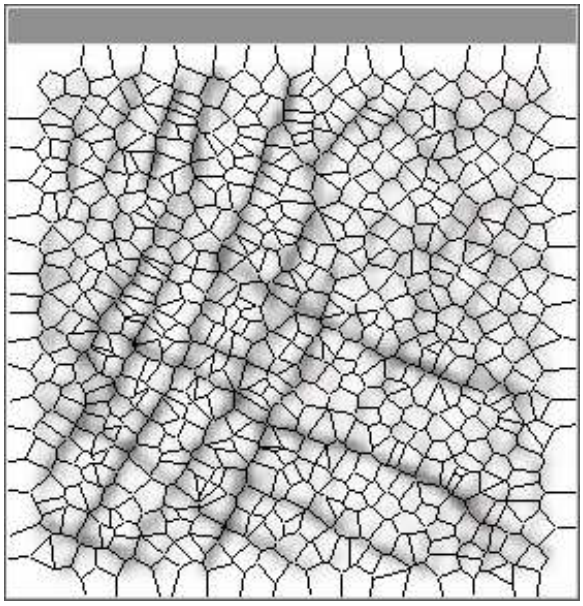

Figure 10: Voronoi polygonal mesh aligned to seismic image.

D. Gibson, M. S. & Turner, J., 2003. Automatic fault detection for 3d seismic data. In *Proceedings of The VII Digital Image Computing: Techniques and Applications*.

Geometry Factory, 2004. CGAL 3.1. Computacional Geometry Algorithms Library.

Gonzales, R. & Woods, R., 1992. *Digital Image Processing*. Addison-Wesley Publishing Company, Inc.

Hale, D., 2001. Atomic images - a method for meshing digital images. In *10th International Meshing Roundtable*, Newport Beach, CA.

Hale, D., 2002. Atomic meshes: from seismic imaging to reservoir simulation. In *Proceedings of the 8th European Conference on the Mathematics of Oil Recovery*, Freiberg, Germany.

Hale, D. & Emanuel, J., 2004. Seismic interpretation using global image segmentation. *Landmark Graphics.*, vol. .

Jalba, A., Wikinson, M., & Roerdink, J., 2004. CPM: A deformable model for shape recovery and segmentation based on charged particles. *IEEE Transactions on Pattern Analysis and Machine Intelligence*, vol. 26, n. 10, pp. 1–16.

Kass, M., Witkin, A., & Terzopoulos, D., 1988. Snakes: Active contour models. *International Journal of Computer Vision*, vol. 1, pp. 321–331.

M. H. Garcia, A. G. J. & Aziz, K., 1992. Automatic grid generation for modeling reservoir heterogeneities. *SPE Reservoir Engineering*, vol. , pp. 278–284.

McInerney, T. & Terzopoulos, D., 1995. Topologically adaptable snakes. In *Proceedings of The International Conference on Computer Vision*, pp. 840–845.

Shimada, K., 1993. Physically-based mesh generation: Automated triangulation of surfaces and volumes via bubble packing. *PhD thesis , Massachusetts Institute of Technology*, vol. .

T. Randen, S. P. & Sonneland, L., 2001. Automatic extraction of fault surfaces from three-dimensional seismic data. *SEG*, vol. .

Ville, D. V. D., T. Blu, M. U., Philips, W., Lemahieu, I., & de Walle, R. V., 2004. Hex-splines: A novel spline family for hexagonal lattices. *IEEE Transactions on Image Processing*, vol. 13, n. 6.

Y. Gdalyahu, D. W. & Werman, M., 2001. Self-organization in vision: Stochastic clustering for image segmentation,perceptual grouping, and image database organization. *IEEE Transactions on Pattern Analysis and Machine Intelligence*, vol. 23, n. 10.